3D phenotyping in a Colombian population reveals unique population and ontogenic facial patterns in genetic and rare disorders

Mireia Andreu-Montoriol[1*], Marina Pujol[1*], Luis Miguel Echeverry-Quiceno[1], Estephania Candelo[2,3], Álvaro Heredia-Lidón[4], Eidith Gómez[2], Paula Solís[2], Diana Ramírez[2], Diana Ortiz[2], Xavier Sevillano[4], Max Rubert Tayà[1], Maria Esther Esteban[1], Aroa Casado[1], Harry Pachajoa[2,3] and Neus Martínez-Abadías[1]

[1] Departament de Biologia Evolutiva, Ecologia i Ciències Ambientals (BEECA), Facultat de Biologia, Universitat de Barcelona (UB), Barcelona, 08028, Spain

[2] Centro de Investigaciones en Anomalías Congénitas y Enfermedades Raras (CIACER), Universidad ICESI, Cali, Colombia.

[3] Servicio de Genética Clínica, Fundación Valle del Lili, Cali, Colombia.

[4] Human-Environment Research Group, La Salle - Universitat Ramon Llull, Barcelona, 08022, Spain.

* First co-authors

ABSTRACT

Up to 30-40% of genetic and rare disorders present with unique facial patterns. Clinical geneticists have traditionally assessed facial traits to suggest a first diagnosis and direct confirmatory genetic testing. However, to enhance the accuracy of early diagnosis using facial biomarkers, it is crucial to analyze the complexity of facial dysmorphologies using 3D technologies, further understand how facial ontogeny is altered within each condition, and broaden the analysis to include diverse human populations.

In this study, we analyzed the 3D facial phenotypes associated to Down (DS), Morquio (MS), Noonan (NS), and Neurofibromatosis type 1 (NF1) syndromes, in an admixed Latin American population from Colombia, including 47 patients and 49 age matched controls. For each subject, we generated a three-dimensional facial model from 2D images captured by a multi-camera photogrammetric system, and recorded the 3D coordinates of 21 anatomical landmarks. Using geometric morphometrics, we characterized the 3D facial dysmorphologies associated with each syndrome and

assessed the range of variation across syndromes as compared to controls. Finally, we tested whether these syndromes alter the ontogenetic trajectory of facial growth.

Our results confirmed statistically significant facial shape differences associated with these genetic conditions, except for NF1. Consistent with our previous 2D analyses, we identified population-specific facial features in the Colombian patients that were not reported in individuals of European descent. Additionally, the pooled 3D analyses revealed a continuous spectrum of facial dysmorphology, with MS exhibiting the most severe dysmorphologies compared to controls. The ontogenic analyses further demonstrated that craniofacial development is altered in DS and MS, but not in RASopathies such as NS and NF1.

Overall, our findings indicate that interpopulation and ontogenic differences in facial phenotypes should be considered to optimize and universalize the use of facial biomarkers. This approach could further help reduce the diagnostic odyssey associated with syndromic and rare conditions.

INTRODUCTION

Genetic syndromes affect 8% of the global population, impacting around 500 million people (Baird et al., 1988; Nguengang et al., 2020). Their frequency varies across populations, but most are rare conditions, affecting fewer than 5 cases in 10,000 people. Despite their low prevalence, there are over 7,000 rare disorders, each associated with a specific pattern of clinical signs and symptoms. Obtaining an early diagnosis is crucial for accurate genetic counseling, effective treatment, and the implementation of prevention strategies (Schieppati et al., 2008). However, the low prevalence of these syndromes, limited understanding of their genetic causes, correlation with other comorbidities, and overlap of clinical symptoms represent significant diagnostic challenges in rare disorders (Schieppati et al., 2008). To address these issues, researchers are exploring alternative methods to complement clinical and molecular diagnostic approaches, which are scarce in the early stages of life (Gülbakan et al., 2016).

The analysis of facial dysmorphologies is currently one of the most promising methods (Gurovich et al., 2019; Hallgrímsson et al., 2020; Hsieh et al., 2022). Between 30-40% of known rare genetic conditions present with unique facial patterns. These traits are

typically congenital and result from alterations in multiple signaling pathways that regulate craniofacial development (Naqvi et al., 2022), including Sonic Hedgehog (SHH), Fibroblast Growth Factor (FGF), Bone Morphogenetic Protein (BMP), Wnt, and Transforming Growth Factor β (TGFβ) (Francis-West et al., 1998; Martínez-Abadías et al., 2011; Richtsmeier et al., 2013; Hallgrímsson et al., 2015). Facial dysmorphologies in genetic and rare disorders range from subtle to severe (Jones et al., 2013) and can provide critical insights to clinical geneticists for disorder diagnosis (Gurovich et al., 2019; Hallgrímsson et al., 2020; Hsieh et al., 2022).

Traditionally, facial dysmorphologies have been assessed to propose an initial diagnosis that guides confirmatory genetic testing. Clinical practice has relied on qualitative descriptions, categorical classifications, and basic quantitative analyses based on anthropometric measurements (Kolar et al., 1987; Aase, 1990; Merks et al., 2003; Reardon & Donnai, 2007). However, the complexity of facial dysmorphologies and the high variability within syndromes make facial assessment challenging, requiring highly trained and experienced specialists (Reardon & Donnai, 2007).

Recently, more sophisticated quantitative methods based on computer vision, machine learning and geometric morphometric techniques have been developed to enable more objective and automatic evaluation of facial morphology (Aponte et al, 2024; Bannister et al., 2020; Gurovich et al., 2019; Hallgrímsson et al., 2020; Hammond et al., 2004; Hammond, 2007; Hammond & Suttie, 2012; Hsieh et al., 2022; Hurst, 2018; Köhler et al., 2019). Methods such as Face2Gene have demonstrated high potential for diagnosing genetic and rare disorders and are routinely used by clinical geneticists in hospitals worldwide (Gurovich et al., 2019; Hsieh et al., 2022). However, current diagnostic algorithms can be further improved to better understand the complex nature of the facial phenotypes associated with genetic and rare disorders.

First, the use of 3D methods can enhance facial biomarker discovery. Most automated diagnostic methods are based on the analysis of 2D photographs (Gurovich et al., 2019), which are amenable to collect but disregard facial depth differences commonly associated with genetic and rare disorders. In comparison, 3D technologies are less accessible but can more efficiently capture the distinct facial patterns specific of each disorder (Hallgrímsson et al., 2020). For instance, recent studies using 3D geometric morphometrics have identified detailed facial patterns associated with rare disorders (Aponte et al., 2024); and very subtle but significant differential facial traits between patients and controls, as in psychotic disorders (Hostalet et al., 2024).

Second, although facial dysmorphologies often originate during embryonic development and continue to evolve throughout an individual's life (Viteri et al., 2020), the impact of growth on facial shape has been minimally explored in rare disorders. Understanding whether a disorder causes significant growth deviations with age is crucial for refining diagnostic and prognostic models.

And third, the limited availability of large-scale datasets for training diagnostic algorithms has led to a predominant reliance on individuals of European descent (Allanson et al., 2009; Hallgrímsson et al., 2020; Masnada et al., 2020). Consequently, African, Asian, and Latin American populations remain underrepresented in diagnostic models. This imbalance is also evident in medical reference texts, where Latin American individuals are notably absent from key resources such as Smith's Recognizable Patterns of Human Malformation (Jones et al., 2013). As a result, diagnostic algorithms based on European-centered reference populations fail to capture the full spectrum of genetic and phenotypic diversity present in other continents or admixed populations. However, accumulating evidence shows that incorporating ancestry diversity in biomedical research improves the discovery and comprehensive mapping of genetic variants associated with anthropometric traits (Fernández-Rhodes et al., 2023), craniofacial shape (Goovaerts et al., 2023) and diseases (Wojcik et al., 2019), and is crucial for further improving current diagnostic models.

In a previous study, we analyzed the facial dysmorphologies associated to genetic and rare disorders in a highly admixed sample comprising pediatric and adult subjects from Colombia using 2D facial data (Echeverry-Quiceno et al., 2023). This initial analysis revealed population-specific traits and highlighted the reduced accuracy of current diagnostic algorithms for rare disorders in this Latin American population compared to European populations (Echeverry-Quiceno et al., 2023). Building on these findings, we are now re-analyzing the facial phenotypes of Down, Morquio, Noonan, and Neurofibromatosis type 1 syndromes in this Colombian population using 3D analysis techniques. Our aim is to achieve improved outcomes by further investigating not only the 3D facial dysmorphologies associated with each syndrome, but also the phenotypic variation across syndromes and the ontogenetic trajectories associated with each of these genetic conditions, which are prevalent in Colombia.

Down syndrome (DS, OMIM 190685) is a genetic condition caused by trisomy of chromosome 21 (Antonarakis et al., 2020), occurring in approximately 1 in every 800

births worldwide (Roper & Reeves, 2006; Bull, 2020). The presence of an extra chromosome leads to a widespread genetic imbalance, resulting in intellectual disability, as well as cardiovascular, respiratory, digestive, and neurological and musculoskeletal issues (Bull, 2020). The craniofacial phenotype of DS is characterized by the presence of brachycephaly and midfacial flattening (Starbuck et al., 2013; Vicente et al., 2020; Starbuck et al., 2021). More specific facial dysmorphologies include oblique palpebral fissures, hypertelorism, broad nose with a depressed nasal bridge, open and small mouth, as well as macroglossia, micrognathia, and a narrow palate, which affect vital functions such as breathing, eating, and speaking (Bull, 2020; Vicente et al., 2020; Starbuck et al., 2021).

Morquio syndrome, also known as mucopolysaccharidosis type IV.A (MS, OMIM 253000) is an autosomal recessive condition with a worldwide prevalence at birth ranging from 1 in 200,000 to 1 in 300,000 live births (Suárez-Guerrero et al., 2015). Colombia presents one of the highest prevalence rates in the world, with 0.68 per 100,000 live births, likely due to founder effects (Pachajoa et al., 2021). Morquio syndrome belongs to a family of disorders characterized by enzymatic deficiencies that lead to the toxic accumulation of intermediate substances in the lysosomes during glycosaminoglycan metabolism. Specifically, MS is caused by mutations in the GALNS gene, which encodes the enzyme responsible for hydrolyzing chondroitin sulfate from N-acetyl-D-galactosamine 6-sulfate and the units of keratan sulfate from D-galactose 6-sulfate (Suárez-Guerrero et al., 2015). Clinical manifestations involve osteoarticular and connective tissue, with accumulation of keratan sulfate in the cartilage and cornea (Uribe et al., 2013). These alterations lead to progressive and permanent damage in fibroblasts that manifest phenotypically as short stature, short neck, protruding thorax, scoliosis and hyperlordosis, joint hyperlaxity, widened and deformed long bones, and a coarse face. Characteristic facial features include frontal protrusion and a flat nasal bridge, thick lips, macroglossia, corneal opacity, glaucoma, and hypertelorism (Obando et al., 2007; Suárez-Guerrero et al., 2015).

Noonan syndrome and Neurofibromatosis type 1 are RASopathies (Denayer & Legius, 2008), caused by alterations in the regulation of the RAS-MAPK intracellular signaling pathway (Roberts et al., 2013). While different conditions share common characteristics, each RASopathy presents unique distinctive features. Noonan syndrome (NS, OMIM 163950) is an autosomal dominant genetic condition with a prevalence of 1 in every 1,000-2,500 live births (Roberts et al., 2013), caused by mutations in the PTPN11 (50%), SOS1 (23%), RAF1 (5%), or KRAS (<5%) genes

(Rauen, 2016). Individuals with NS present mild intellectual disability and hearing loss, cardiac problems and skin pigmentation alterations (melanocytic nevi, CAL spots, and benign pigmented macular lesions). Skeletal malformations include short stature, chest malformations, hand and vertebral anomalies (Lee et al., 2019). Facially, individuals with NS present a wide forehead, hypertelorism, ptosis, epicanthic folds, and a lip margin with an accentuated upward angulation (Hernández-Martín et al., 2011). Other features include arched eyebrows, a wide neck, low hair implantation along the posterior hairline and low-set ears with posterior rotation (Cremers et al., 1992).

Neurofibromatosis type 1 (NF1, OMIM 162200) is an autosomal disorder associated with dermatological, cardiovascular, gastrointestinal, and skeletal implications, with a worldwide prevalence of 1 in 4,000 live births. The loss of the tumor suppressor gene known as neurofibromin 1, which acts as a negative regulator of RAS proteins, is responsible for this condition, although environmental factors also significantly influence the phenotypic expression of this syndrome (Pasmant et al., 2012). The most characteristic clinical features of NF1 include axillary freckling, Lisch nodules, optic pathway gliomas, CAL spots, and tumors of the optic nerve sheath (Pasmant et al., 2012). Dysplasia of long bones, autism, and pheochromocytoma have been identified as unique traits of NF1 within the family of neurofibromatosis (Cimino et al., 2018). Facially, macrocephaly, proptosis caused by the agenesis of the greater wing of the sphenoid and by the effect of optic pathway gliomas, maxillary and mandibular deformities, as well as dental anomalies can be observed (Chauvel-Picard et al., 2020).

The clinical manifestations associated with these genetic and rare disorders are known to vary across population ancestry (Kruszka et al. 2017a, b, c; Echeverry-Quiceno et al, 2023). The objective of this study is to more precisely quantify the 3D facial shape dysmorphology patterns associated with DS, MS, NS and NF1 in an admixed Colombian population. We compared groups of patients and controls using 3D geometric morphometrics to define the specific and ontogenic facial morphological patterns associated with these syndromic conditions. Our hypothesis is that by deepening our understanding of the distinctive facial phenotype in this admixed population, our results will contribute to an earlier, more accurate and non-biased diagnosis, ultimately supporting a future approach to personalized clinical management.

MATERIALS AND METHODS

Population sample

The sample was collected in 2021 in Cali (Colombia) (Echeverry-Quiceno et al, 2023) and comprised 96 individuals from both sexes ranging from 2 to 51 years old (Table 1). The cohort included 49 age matched controls recruited at University ICESI and Colegio Ecológico Scout, and 47 people diagnosed with Down, Morquio, Noonan and Neurofibromatosis type 1 syndromes that were recruited from the clinical genetics consultation at Hospital-Fundación Valle del Lili in Cali (Colombia), a tertiary health reference center for these genetic and rare disorders (Table 1). Clinical diagnoses were confirmed by molecular genetic testing.

Table 1: Cohort composition by diagnostic groups and sex.

Syndrome	Female	Male	Total
Down	11	8	19
Morquio	5	3	8
Noonan	5	3	8
Neurofibromatosis type 1	6	6	12
PATIENTS	27	20	47
CONTROL	34	15	49
TOTAL	61	35	**96**

The study was approved by the “Ethics Committee for Human Research at Universidad Icesi” with approval record no. 309, and complied with the national guidelines and protocols. All participants signed informed consent forms to participate in the study. For minor children, the informed consent was obtained from the parents or legal guardians to acquire facial photographs and associated clinical information.

Acquisition of facial images and collection of anatomical landmarks

The methodology for acquiring facial data was based on photogrammetry techniques, a non-invasive, efficient, and cost-effective tool for creating high-resolution three-dimensional (3D) models and obtaining reliable measurements (Hallgrímsson et al 2020; Starbuck et al., 2021). We employed photographic equipment consisting of 10 synchronized digital cameras (SONY Alpha 58 +18-55) mounted on 5 tripods at two different heights, arranged in a semicircle one meter away from the subject (Starbuck et al., 2021). The cameras were triggered simultaneously using a remote control, capturing subjects from various angles and positions. To ensure a natural facial

expression, images were taken with the subjects in an upright position and a neutral facial expression. Multiple photographs were taken for each individual, and the optimal shot was selected for facial reconstruction. By superimposing overlapping 2D images, common cloud points were detected through triangulation, and 3D facial surface meshes and textures were generated using AgiSoft PhotoScan. The facial meshes were then scaled and stored as ply files.

To measure the facial shape of each individual and detect the traits associated with DS, MS, NS, and NF1, we recorded the 3D coordinates of 21 anatomical facial landmarks (Figure 1 and Supplementary Table 1) using 3DSlicer 5.0.2 (Fedorov et al., 2012). Landmarks were acquired manually by the same observer after landmarking training to reduce intra-observer measurement error. A subsample of 25 individuals, including five subjects from each group, were measured five times with a 48-hour interval between each measurement. Quantitative tests showed that variation within individuals due to intra-observer error was significantly lower than biological variation between individuals (p-value <0.010), and the mean measurement error was below 2 mm. Since this error threshold is widely accepted in studies of biological anthropology for craniometric measurements (Stull et al., 2014), the landmarks reliability was validated for both control and syndromic samples. Following inspection of landmark coordinates for gross error, anatomical landmark coordinates were used to conduct morphometric analyses.

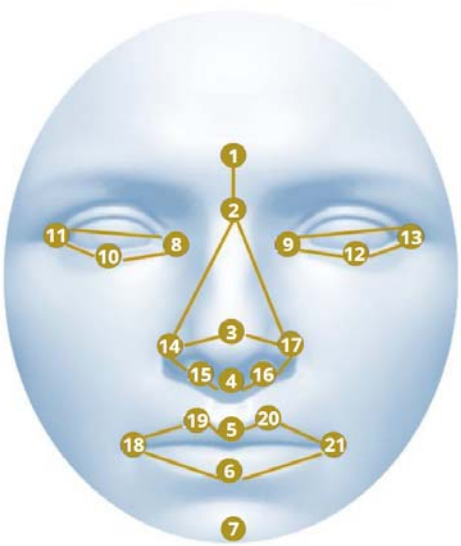

Figure 1. 3D facial reconstruction showing the location of the analyzed 21 anatomical landmarks (round numerical symbols). Anatomical landmark definitions are provided in Supplementary Table 1.

Quantitative facial shape analyses

First, we assessed the facial shape differences within each syndrome. For each pair of control/patient groups, we performed a Generalized Procrustes Analysis (GPA) based on the 3D Cartesian coordinates of the 21 facial landmarks (Dryden & Mardia, 1998). The landmark configurations of all individuals were superimposed by shifting them to a common position, scaling to a standard size, and rotating them until a least square best fit was achieved between homologous landmarks (Dryden & Mardia, 1998).

The resulting Procrustes coordinates were then used to perform a Principal Component Analysis (PCA). Facial variation within each syndrome was represented by creating a morphospace based on the first two principal components (PCs). If slight or no facial dysmorphologies were associated with the syndrome, the control and patient groups overlapped in the PCA scatterplot, showing similar phenotypes. If there were shape differences, the groups separated from each other in the morphospace, showing distinct facial phenotypes. To quantitatively assess the facial differences between patients and controls, we estimated the Procrustes distances between pairs groups as the square root of the sum of squared differences between respective landmarks in the two mean shapes after Procrustes superimposition (Klingenberg 2016). To test whether the facial shape differences were statistically significant, we ran permutation tests with 1,000 iterations.

After assessing the facial shape differences in DS, MS, NS, and NF1 individually, we explored the overall facial shape variation across these syndromes. To do this, we conducted a Generalized Procrustes Analysis (GPA) and a Principal Component Analysis (PCA) by pooling all samples together.

Finally, to analyze the effects of growth and ontogeny and to test whether the genetic disorders alter the expected trajectories, we performed multivariate regressions of facial shape on facial size and individual age (Klingenberg, 2016). Facial size was measured as centroid size, a common measure in geometric morphometrics, computed as the square root of the sum of squared distances of all the facial landmarks from the centroid (Mitteroecker & Gunz, 2009). If a statistically significant influence of facial size was detected, the Procrustes distances among pairs of groups were recalculated

based on the regression residuals. All morphometric and statistical analyses were performed with MorphoJ (Klingenberg, 2011).

RESULTS

The PCA results exploring facial shape variation in genetic and rare syndromes showed separation along PC1 between controls and patients diagnosed with DS, MS and NS, but not for NF1 (Figure 2). The facial changes associated with Down syndrome (Figure 2a) included a wider and flattened face, oblique palpebral fissures, hypertelorism, a depressed nasal bridge, and a wide nose with a large distance between the alae (Figure 2a). Additionally, mandibular prognathism and thicker upper lips were detected. The analysis of Procrustes distances confirmed that the facial shape differences in DS were statistically significant (Procrustes distances: 0.0801; p-value: <.0001).

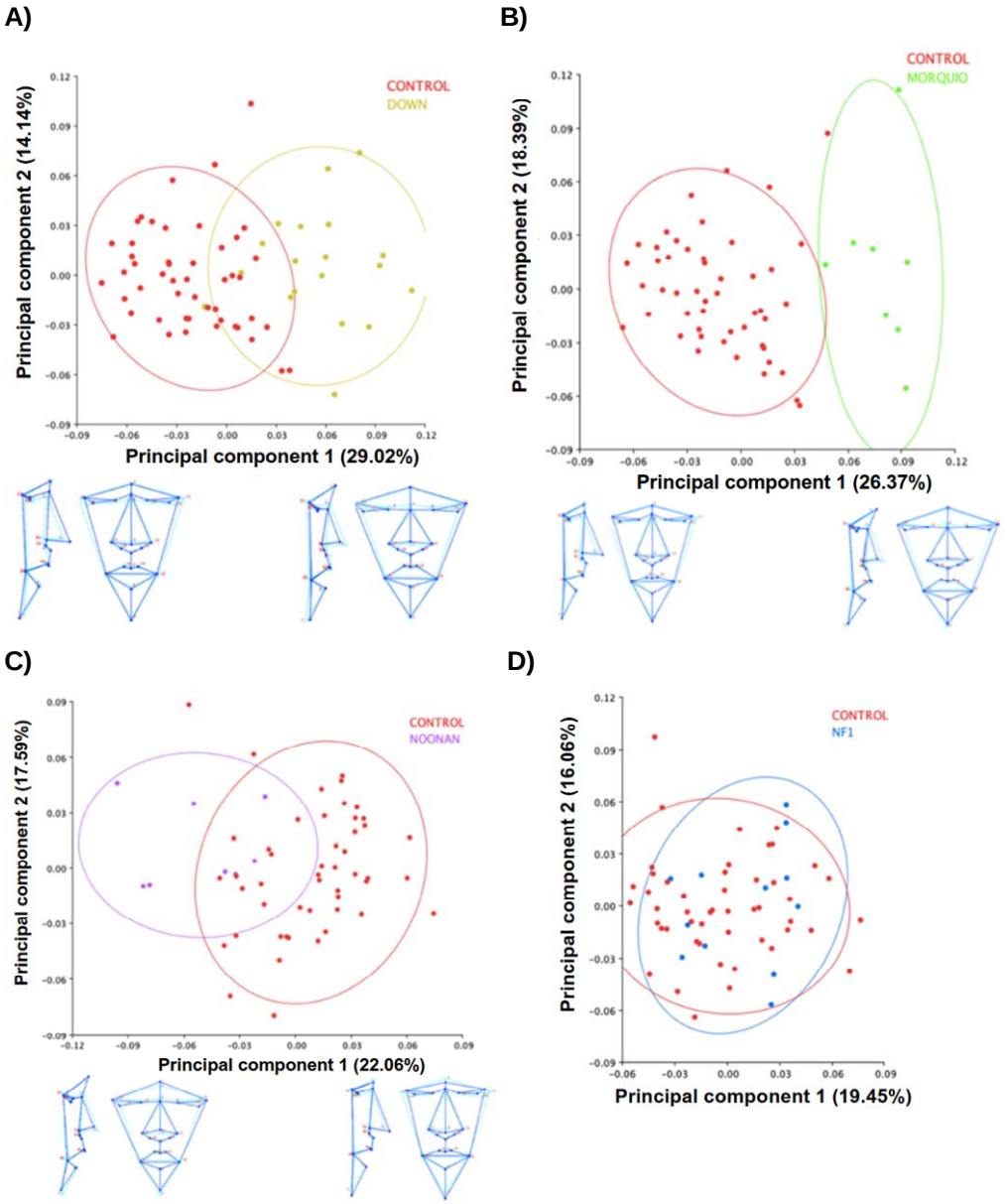

Figure 2. Results of the Principal Component Analyses (PCA) comparing controls with individuals diagnosed with DS (A), MS (B), NS (C) and NF1 (D). Ellipses show 90% confidence interval of facial shape variation within each group. The wireframes represent lateral and frontal views of the facial shape changes along PC1. The light blue wireframe represents the average shape, while the dark blue wireframe displays the shape associated with the negative (left) and positive (right) extremes of variation in PC1.

Results indicated that Morquio syndrome was associated with the most severe dysmorphologies, as no overlap was detected between patients and controls (Figure 2b), and the Procrustes distance was the highest among all comparisons (Procrustes distances: 0.0943; p-value: <.0001). The facial features associated with MS included

facial retrusion, larger distance between the eyes, depression of the nasal bridge, a protruding forehead, and a thicker upper lip (Figure 2b).

The facial shape differences associated with Noonan syndrome were also statistically significant (Procrustes distances: 0.0683; p-value: <.0001), but the least severe among the analyzed conditions, since the PCA showed a larger overlap between controls and individuals diagnosed with NS (Figure 2c), and the Procrustes distance was the smallest among comparisons. Individuals with NS exhibited a longer and narrower face, mandibular retrognathism, and thick lips (Figure 2c).

Neurofibromatosis type 1 was the only syndrome that did not show facial differences between controls and patients. The PCA showed a complete overlap between individuals, indicating no characteristic facial features associated with NF1 (Figure 2d). The Procrustes distances confirmed that the differences were not statistically significant (Procrustes distances: 0.0212; p-value: 0.6719).

We also explored the facial morphological variation of all syndromic groups in relation to the control sample (Figure 3). The morphospace defined by the first 2 PCs explained 42.24% of total facial shape variation and showed substantial overlap among groups. However, the positioning of individuals along PC1 revealed a continuous range of variation in facial dysmorphology. Cntrol individuals were located at the negative extreme of PC1, overlapping with NF1-diagnosed individuals, who previously showed no significant facial dysmorphologies (Figure 3). Individuals with NS were located in the middle of the morphospace, partially overlapping with controls, NF1 and DS individuals with moderate dysmorphologies. At the positive extreme of PC1, we found individuals with DS and more severe dysmorphologies, as well as individuals diagnosed with MS, who showed the greatest dispersion along PC2 and were the only group completely separated from controls (Figure 3).

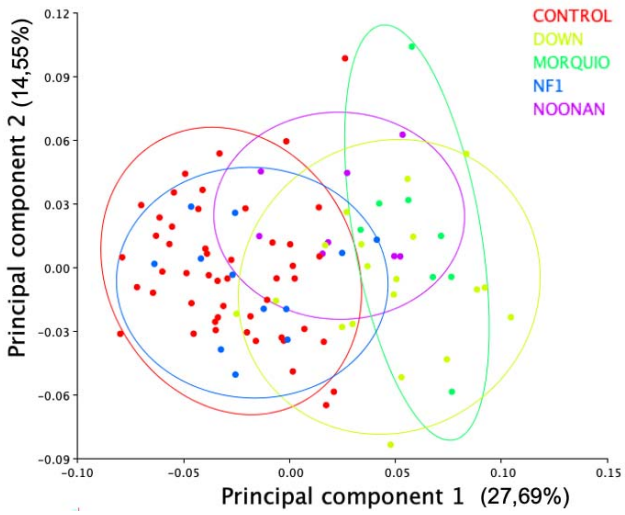

Figure 3. Results of the Principal Component Analysis (PCA) based on the pooled sample of individuals diagnosed with DS, MS, NS, NF1 along with the control sample, showing a continuous range of facials shape variation. Ellipses show 90% confidence interval of facial shape variation within each group.

When we assessed the influence of facial size on shape, we detected a significant allometric effect (p-value <0.0001). The multivariate linear regression between the Procrustes coordinates and centroid size was significant, with facial size explaining 15.4% of the total facial shape variation. To determine whether the facial dysmorphologies revealed by the previous analyses were maintained after removing the allometric effect, we calculated the Procrustes distances between the groups from the regression residuals. The results confirmed significant facial shape differences between controls and individuals diagnosed with DS, MS and NS, and further indicated non-allometric morphological differences in individuals with these syndromic conditions (Table 2).

	CONTROL	DS	MS	NS
DS	0.046			
	<.0001			
MS	0.0872	0.0679		
	<.0001	*<.0001*		
NS	0.0452	0.0648	0.0772	
	0.0023	*<.0001*	*<.0001*	
NF1	0.0208	0.0392	0.0815	0.0449

	0.6158	*0.0291*	*<.0001*	*0.0084*

Table 2: Procrustes distances between groups with associated p-values, based on the residuals of the multivariate regression of facial shape on centroid size.

Finally, the multivariate linear regression of facial shape on age indicated a significant positive correlation, with age explaining 9.7% of facial morphological variation (p-value <0.0001). The ontogenetic trajectories associated with NS and NF1 were parallel to the control group, showing no altered growth patterns in individuals with RASopathies (Figure 5). However, the trajectories associated with DS and MS showed non-parallel slopes compared to controls, suggesting deviations in facial growth patterns in these syndromic conditions.

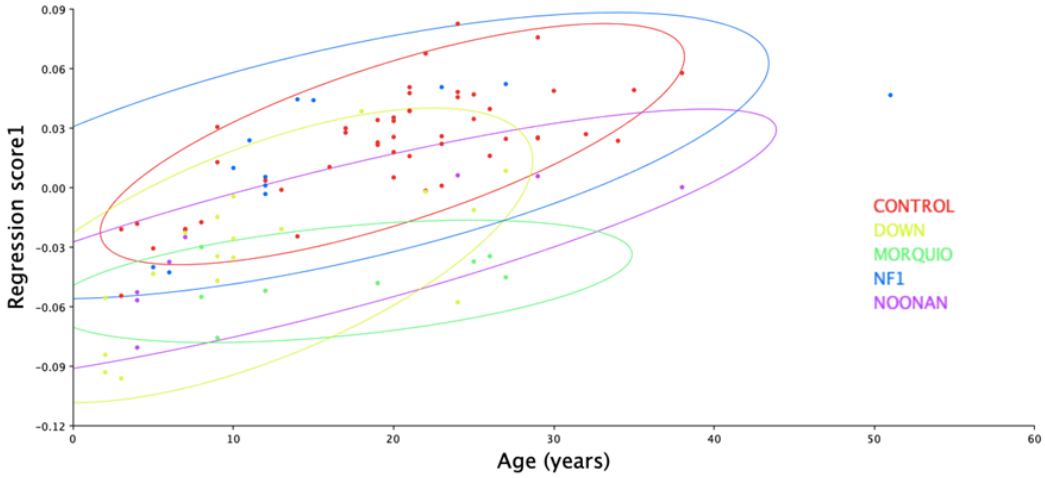

Figure 5. Ontogenetic trajectories assessed by multivariate linear regression of facial shape on age. Ellipses show 90% confidence interval of facial shape variation within groups.

DISCUSSION

This study extends our previous analysis of facial dysmorphologies linked to genetic and rare conditions, including DS, MS, NS, and NF1, within a Colombian population (Echeverry-Quiceno et al., 2023). The use of 3D geometric morphometric methods for analyzing facial dysmorphologies represents a significant advancement over qualitative and 2D descriptions of facial variation. These methods provide a more precise quantitative tool to detect facial shape differences between patients and controls, while controlling for significant factors such as facial size and age (Hallgrímsson et al., 2015). Consequently, 3D methods enhance the potential use of facial biomarkers for

diagnosis and prognosis of genetic and rare disorders (Aponte et al, 2024; Bannister et al., 2020; Gurovich et al., 2019; Hallgrímsson et al., 2020; Hammond et al., 2004; Hammond, 2007; Hammond & Suttie, 2012; Hsieh et al., 2022; Hurst, 2018; Köhler et al., 2019).

By analyzing the facial dysmorphologies in an admixed population, our results confirmed that despite sharing the common pattern of facial dysmorphology described in the literature, Colombian subjects also present population-specific traits for each syndrome. these traits are likely due to the diverse genetic ancestry of the Colombian population (Echeverry-Quiceno et al., 2023). Historical records report that the Cali region has been shaped by diverse migratory processes (Urrea-Giraldo et al., 2017), and the current population is characterized by indigenous and mestizo communities. Admixture with the indigenous Amerindian population began in the sixteenth century with the arrival of Spanish colonizers. In the eighteenth century, the establishment of large colonial settlements of African slaves for sugar cane exploitation significantly altered the population structure of Valle del Cauca (Urrea-Giraldo et al., 2017). Nowadays, the Amerindian and African ancestry predominate in this Colombian region over European ancestry (Adhikari et al., 2017).

Regarding the facial dysmorphologies associated with DS, the features observed in our Colombian sample are consistent with those described in the populations of European descent described in the literature (Antonarakis et al., 2020; Bull, 2020; Starbuck et al., 2013; Starbuck et al., 2021). However, in our Colombian sample, a thicker upper lip compared to the lower lip was also detected as a characteristic feature of individuals with DS. Similarly, in MS, all the traits mentioned by Suárez-Guerrero et al. (2020) were observed, as well as the difference in lip thickness already observed in DS.

Our results of the facial analysis of NS diverged substantially from the descriptions found in the literature (Hernández-Martín et al., 2011) based on a European population, since individuals diagnosed with NS in the Colombian sample exhibited mandibular retrognathism and thick lips. Regarding NF1, no significant differences were found. As previous studies have shown (Chauvel-Picard et al., 2020), both Colombian and European populations only display subtle facial features that do not reach statistical significance when comparing patients to controls.

The 3D morphometric analyses performed in this study confirmed unique and differential patterns in the facial morphology of DS, MS, and NS, except for NF1. When

we assessed the facial patterns in RASopathies, the results indicated statistically significant differences. Despite previous studies suggesting that RASopathies present shared facial dysmorphologies (Denayer & Legius, 2008), our results confirmed that NS and NF1 can be distinguished based on their facial phenotypes.

The analysis pooling all the subjects with syndromic conditions revealed a continuous spectrum of facial shape variation. NS exhibited low to moderate facial dysmorphologies, whereas DS showed moderate to more severe dysmorphologies, and MS exhibited the most severe facial dysmorphologies. These results are consistent with our previous findings based on 2D facial shape analyses (Echeverry-Quiceno et al., 2023), but extend the results covering the 3D shape of the face and further reveal allometric effects in facial shape variation.

Finally, we assessed the differences in the ontogenetic trajectory of each syndrome compared to controls to quantify the facial morphological variation throughout postnatal development. This aspect of facial shape variation has not been thoroughly investigated before but is crucial for understanding the natural history of genetic and rare conditions and providing the basis to develop reliable prognostic methods (Liu et al., 2022). Our results indicated that the trajectories associated with NS and NF1 were parallel to the control sample; whereas the ontogenetic trajectories of DS and MS were deviated, indicating alterations in their postnatal growth. In particular, the alteration detected in MS is consistent with previous evidence describing that, in mucopolysaccharidosis syndromes, facial dysmorphologies of MS are cumulative and increase over lifetime (Suárez-Guerrero et al., 2015). Further analyses with larger samples are needed to confirm whether adult individuals with MS present more severe facial dysmorphologies than children. Overall, these results underscore the need to specifically assess ontogeny to improve the prognosis and clinical management of individuals with genetic and rare disorders.

CONCLUSIONS

We conclude that there are significant diagnostic and prognostic patterns based on facial dysmorphologies for DS, MS and NS syndromes, but that these patterns need to account for ontogenic and interpopulation differences to reach their maximum potential and be used worldwide in diverse human populations.

BIBLIOGRAPHY

Aase, J.M. (1990) The physical examination in dysmorphology in diagnostic dysmorphology (ed. Plenum Medical Book Company) 33–42 (New York and London).

Adhikari, K., Chacón-Duque, J. C., Mendoza-Revilla, J., Fuentes-Guajardo, M. & Ruiz-Linares, A. (2017) The genetic diversity of the Americas. Annual Review of Genomics and Human Genetics, 18, 277–296.

Allanson, J. E., Cunniff, C., Hoyme, H. E., McGaughran, J., Muenke, M., & Neri, G. (2009). Elements of morphology: standard terminology for the head and face. American Journal of Medical Genetics Part A, 149(1), 6-28.

Antonarakis, S. E., Skotko, B. G., Rafii, M. S., Strydom, A., Pape, S. E., Bianchi, D. W., Sherman, S. L., & Reeves, R. H. (2020). Down syndrome. Nature Reviews Disease Primers, 6(1), 1–20

Aponte, J. D., Bannister, J. J., Hoskens, H., Matthews, H., Katsura, K., Da Silva, C., Cruz, T., Pilz, J. H. M., Spritz, R. A., Forkert, N. D., Claes, P., Bernier, F. P., Klein, O. D., Katz, D. C., & Hallgrímsson, B. (2024). An interactive atlas of three-dimensional syndromic facial morphology. American Journal of Human Genetics, 111(1), 39–47.

Baird, P. A., Anderson, T., Newcombe, H. & Lowry, R. Genetic disorders in children and young adults: a population study. (1988). American Journal of Human Genetics 42, 677–693.

Bannister, J. J., Crites, S. R., Aponte, J. D., Katz, D. C., Wilms, M., Klein, O. D., Bernier, F. P. J., Spritz, R. A., Hallgrímsson, B., & Forkert, N. D. (2020). Fully Automatic Landmarking of Syndromic 3D Facial Surface Scans Using 2D Images. Sensors (Basel, Switzerland), 20(11)

Bull, M. J. (2020). Down syndrome. New England Journal of Medicine, 382(24), 2344-2352.

Chauvel-Picard, J., Lion-Francois, L., Beuriat, P. A., Paulus, C., Szathmari, A., Mottolese, C., ... & Di Rocco, F. (2020). Craniofacial bone alterations in patients with neurofibromatosis type 1. Child's Nervous System, 36(10), 2391-2399.

Cimino, P. J., & Gutmann, D. H. (2018). Neurofibromatosis type 1. Handbook of Clinical Neurology, 148, 799-811.

Cremers, C. W. R. J., & Van der Burgt, C. J. A. M. (1992). Hearing loss in Noonan syndrome. International Journal of Pediatric Otorhinolaryngology, 23(1), 81-84.

Denayer, E. & Legius, E. (2008). Neurofibromatosis Type 1-Noonan Syndrome: What's the Link? In: Noonan Syndrome and Related Disorders-A Matter of Deregulated Ras Signaling (Vol. 17, pp. 128-137). Karger Publishers.

Dryden, I. L., & Mardia, K. V. (1998). Statistical Shape Analysis (1st edition). Wiley.

Echeverry-Quiceno, L. M., Candelo, E., Gómez, E., Solís, P., Ramírez, D., Ortiz, D., González, A., Sevillano, X., Cuéllar, J. C., Pachajoa, H., & Martínez-Abadías, N. (2023). Population-specific facial traits and diagnosis accuracy of genetic and rare diseases in an admixed Colombian population. Scientific Reports, 13(6869).

Fedorov A., Beichel R., Kalpathy-Cramer J., Finet J., Fillion-Robin J-C., Pujol S., Bauer C., Jennings D., Fennessy F., Sonka M., Buatti J., Aylward S.R., Miller J.V., Pieper S., Kikinis R. (2012) 3D Slicer as an Image Computing Platform for the Quantitative Imaging Network. Magnetic Resonance Imaging. Nov;30(9):1323-41.

Francis-West, P., Ladher, R., Barlow, A., & Graveson, A. (1998). Signalling interactions during facial development. Mechanisms of Development, 75(1-2), 3-28.

Fernández-Rhodes, L., Graff, M., Buchanan, V. L., Justice, A. E., Highland, H. M., Guo, X., Zhu, W., Chen, H.-H., Young, K. L., Adhikari, K., Palmer, N. D., Below, J. E., Bradfield, J., Pereira, A. C., Glover, L., Kim, D., Lilly, A. G., Shrestha, P., Thomas, A. G., … North, K. E. (2022). Ancestral diversity improves discovery and fine-mapping of genetic loci for anthropometric traits-The Hispanic/Latino Anthropometry Consortium. HGG Advances, 3(2), 100099.

Goovaerts, S., Hoskens, H., Eller, R. J., Herrick, N., Musolf, A. M., Justice, C. M., Yuan, M., Naqvi, S., Lee, M. K., Vandermeulen, D., Szabo-Rogers, H. L., Romitti, P. A., Boyadjiev, S. A., Marazita, M. L., Shaffer, J. R., Shriver, M. D., Wysocka, J., Walsh, S., Weinberg, S. M., & Claes, P. (2023). Joint multi-ancestry and admixed GWAS reveals the complex genetics behind human cranial vault shape. Nature Communications, 14(1), 7436

Gülbakan, B., Özgül, R. K., Yüzbaşıoğlu, A., Kohl, M., Deigner, H. P., & Özgüç, M. (2016). Discovery of biomarkers in rare diseases: innovative approaches by predictive and personalized medicine. The EPMA journal, 7(1), 24.

Gurovich, Y., Hanani, Y., Bar, O., Nadav, G., Fleischer, N., Gelbman, D., ... & Gripp, K. W. (2019). Identifying facial phenotypes of genetic disorders using deep learning. Nature Medicine, 25(1), 60-64.

Hallgrímsson, Benedikt & Percival, Christopher & Green, Rebecca & Young, Nathan & Mio, Washington & Marcucio, Ralph. (2015). Morphometrics, 3D Imaging, and Craniofacial Development. Current Topics in Developmental Biology. 115. 561-597.

Hallgrímsson, B., Aponte, J. D., Katz, D. C., Bannister, J. J., Riccardi, S. L., Mahasuwan, N., ... & Klein, O. D. (2020). Automated syndrome diagnosis by three-dimensional facial imaging. Genetics in Medicine, 22(10), 1682-1693.

Hammond, P., Hutton, T. J., Allanson, J. E., Campbell, L. E., Hennekam, R. C., Holden, S., Patton, M. A., Shaw, A., Temple, I. K., Trotter, M., Murphy, K. C., & Winter, R. M. (2004). 3D analysis of facial morphology. American Journal of Medical Genetics. Part A, 126A(4), 339–348.

Hammond P. (2007). The use of 3D face shape modelling in dysmorphology. Archives of Disease in Childhood, 92(12), 1120–1126.

Hammond, P., & Suttie, M. (2012). Large-scale objective phenotyping of 3D facial morphology. Human Mutation, 33(5), 817–825.

Hernández-Martín, A., & Torrelo, A. (2011). Rasopatías: trastornos del desarrollo con predisposición al cáncer y manifestaciones cutáneas. Actas Dermo-Sifiliográficas, 102(6), 402-416.

Hostalet, N., González, A., Salgado-Pineda, P., Gonzàlez-Colom, R., Canales-Rodríguez, E. J., Aguirre, C., Guerrero-Pedraza, A., Llanos-Torres, M., Salvador, R., Pomarol-Clotet, E., Sevillano, X., Martínez-Abadías, N., & Fatjó-Vilas, M. (2024). Face-brain correlates as potential sex-specific biomarkers for schizophrenia and bipolar disorder. Psychiatry Research, 339, 116027.

Hurst A. C. E. (2018). Facial recognition software in clinical dysmorphology. Current Opinion in Pediatrics, 30(6), 701–706.

Hsieh, T. C., Bar-Haim, A., Moosa, S., Ehmke, N., Gripp, K. W., Pantel, J. T., Danyel, M., Mensah, M. A., Horn, D., Rosnev, S., Fleischer, N., Bonini, G., Hustinx, A., Schmid, A., Knaus, A., Javanmardi, B., Klinkhammer, H., Lesmann, H., Sivalingam, S., Kamphans, T., … Krawitz, P. M. (2022). GestaltMatcher facilitates rare disease matching using facial phenotype descriptors. Nature Genetics, 54(3), 349–357.

Jones, K.L., Jones, M.C., & Campo, M. (2013). Smith's recognizable patterns of human malformation (ed. Elsevier Health Sciences)

Klingenberg, C. P. (2011). MorphoJ: an integrated software package for geometric morphometrics. Molecular Ecology Resources 11: 353-357.

Klingenberg, C. P. (2016). Size, shape, and form: concepts of allometry in geometric morphometrics. Development Genes and Evolution, 226(3), 113-137.

Kolar, J. C., Munro, I. R., & Farkas, L. G. (1987). Anthropometric evaluation of dysmorphology in craniofacial anomalies: Treacher Collins syndrome. American Journal of Physical Anthropology, 74(4), 441–451.

Köhler, S., Carmody, L., Vasilevsky, N., Jacobsen, J. O. B., Danis, D., Gourdine, J. P., Gargano, M., Harris, N. L., Matentzoglu, N., McMurry, J. A., Osumi-Sutherland, D., Cipriani, V., Balhoff, J. P., Conlin, T., Blau, H., Baynam, G., Palmer, R., Gratian, D., Dawkins, H., Segal, M., … Robinson, P. N. (2019). Expansion of the Human Phenotype Ontology (HPO) knowledge base and resources. Nucleic Acids Research, 47(D1), D1018–D1027.

Kruszka, P., Addissie, Y. A., McGinn, D. E., Porras, A. R., Biggs, E., Share, M., Crowley, T. B., Chung, B. H. Y., Mok, G. T. K., Mak, C. C. Y., Muthukumarasamy, P., Thong, M.-K., Sirisena, N. D., Dissanayake, V. H. W., Paththinige, C. S., Prabodha, L. B. L., Mishra, R., Shotelersuk, V., Ekure, E. N., … Muenke, M. (2017a). 22q11.2 deletion syndrome in diverse populations. American Journal of Medical Genetics. Part A, 173(4), 879–888.

Kruszka, P., Porras, A. R., Addissie, Y. A., Moresco, A., Medrano, S., Mok, G. T. K., Leung, G. K. C., Tekendo-Ngongang, C., Uwineza, A., Thong, M.-K., Muthukumarasamy, P., Honey, E., Ekure, E. N., Sokunbi, O. J., Kalu, N., Jones, K. L., Kaplan, J. D., Abdul-Rahman, O. A., Vincent, L. M., … Muenke, M. (2017b). Noonan syndrome in diverse populations. American Journal of Medical Genetics. Part A, 173(9), 2323–2334.

Kruszka, P., Porras, A. R., Sobering, A. K., Ikolo, F. A., La Qua, S., Shotelersuk, V., Chung, B. H. Y., Mok, G. T. K., Uwineza, A., Mutesa, L., Moresco, A., Obregon, M. G., Sokunbi, O. J., Kalu, N., Joseph, D. A., Ikebudu, D., Ugwu, C. E., Okoromah, C. A. N., Addissie, Y. A., … Muenke, M. (2017c). Down syndrome in diverse populations. American Journal of Medical Genetics Part A, 173(1), 42–53.

Lee, B. H., & Yoo, H. W. (2019). Noonan syndrome and RASopathies: Clinical features, diagnosis and management. Journal of Genetic Medicine, 16(1), 1-9.

Liu, J., Barrett, J. S., Leonardi, E. T., Lee, L., Roychoudhury, S., Chen, Y., & Trifillis, P. (2022). Natural History and Real-World Data in Rare Diseases: Applications, Limitations, and Future Perspectives. Journal of Clinical Pharmacology, 62(Suppl 2), S38–S55.

Martínez-Abadías, N., Heuzé, Y., Wang, Y., Jabs, E. W., Aldridge, K., & Richtsmeier, J. T. (2011). FGF/FGFR signaling coordinates skull development by modulating magnitude of morphological integration: evidence from Apert syndrome mouse models. PloS one, 6(10), e26425.

Masnada, S., Gibelli, D., Dolci, C., De Giorgis, V., Cappella, A., Veggiotti, P., ... & Italian Aicardi Study Group. (2020). 3D facial morphometry in Italian patients

affected by Aicardi syndrome. American Journal of Medical Genetics Part A, 182(10), 2325-2332.

Merks, J. H., van Karnebeek, C. D., Caron, H. N., & Hennekam, R. C. (2003). Phenotypic abnormalities: terminology and classification. American Journal of Medical Genetics. Part A, 123A(3), 211–230.

Nguengang Wakap, S., Lambert, D. M., Olry, A., Rodwell, C., Gueydan, C., Lanneau, V., Murphy, D., Le Cam, Y., & Rath, A. (2020). Estimating cumulative point prevalence of rare diseases: analysis of the Orphanet database. European Journal of Human Genetics: EJHG, 28(2), 165–173.

Naqvi, S., Hoskens, H., Wilke, F., Weinberg, S. M., Shaffer, J. R., Walsh, S., ... & Claes, P. (2022). Decoding the Human Face: Challenges and Progress in Understanding the Genetics of Craniofacial Morphology. Annual Review of Genomics and Human Genetics. 23(1), 383–412.

Obando, F. S., & Montoya, I. Z. (2007). Aspectos clínicos y manejo integral del síndrome de Morquio. Universitas Médica, 48(2), 166-174.

Pachajoa, H., Acosta, M. A., Alméciga-Díaz, C. J., Ariza, Y., Diaz-Ordoñez, L., Caicedo-Herrera, G., Cuartas, D., Nastasi-Catanese, J. A., Ramírez-Montaño, D., Silva, Y. K., Moreno, L., Satizabal, J., Garcia, N., Montoya, J., Prada, C., Porras, G., Velasco, H., & Candelo, E. (2021). Molecular characterization of mucopolysaccharidosis type IVA patients in the Andean region of Colombia. American Journal of Medical Genetics. Part C, Seminars in Medical Genetics, 187(3), 388–395.

Pasmant, E., Vidaud, M., Vidaud, D., & Wolkenstein, P. (2012). Neurofibromatosis type 1: from genotype to phenotype. Journal of Medical Genetics, 49(8), 483-489.

Rauen, K. A. (2016). Cardiofaciocutaneous syndrome. GeneReviews®.

Reardon, W., & Donnai, D. (2007). Dysmorphology demystified. Archives of Disease in Childhood. Fetal and Neonatal Edition, 92(3), F225–F229.

Richtsmeier, J. T., & Flaherty, K. (2013). Hand in glove: brain and skull in development and dysmorphogenesis. Acta Neuropathologica, 125(4), 469–489.

Roberts, A. E., Allanson, J. E., Tartaglia, M., & Gelb, B. D. (2013). Noonan syndrome. The Lancet, 381(9863), 333-342.

Roper, R. J., & Reeves, R. H. (2006). Understanding the basis for Down syndrome phenotypes. PLoS Genetics, 2(3), e50.

Schieppati, A., Henter, J. I., Daina, E., & Aperia, A. (2008). Why rare diseases are an important medical and social issue. Lancet, 371(9629), 2039–2041.

Starbuck, J. M., Cole, T. M., 3rd, Reeves, R. H., & Richtsmeier, J. T. (2013). Trisomy 21 and facial developmental instability. American Journal of Physical Anthropology, 151(1), 49–57.

Starbuck, J. M., Llambrich, S., Gonzàlez, R., Albaigès, J., Sarlé, A., Wouters, J., ... & Martínez-Abadías, N. (2021). Green tea extracts containing epigallocatechin-3-gallate modulate facial development in Down syndrome. Scientific Reports, 11(1), 1-13.

Stull, K. E., Tise, M. L., Ali, Z., & Fowler, D. R. (2014). Accuracy and reliability of measurements obtained from computed tomography 3D volume rendered images. Forensic Science International, 238, 133–140.

Suárez-Guerrero, J. L., Higuera, P. J. I. G., Flórez, J. S. A., & Contreras-García, G. A. (2016). Mucopolisacaridosis: características clínicas, diagnóstico y de manejo. Revista Chilena de Pediatría, 87(4), 295-304.

Uribe, A., & Giugliani, R. (2013). Selective screening for lysosomal storage diseases with dried blood spots collected on filter paper in 4,700 high-risk colombian subjects. In JIMD Reports-Volume 11 (pp. 107-116). Springer, Berlin, Heidelberg.

Urrea-Giraldo, F. & Álvarez, A. F. C. Cali an enlarged region city: an approximation from the ethnic-racial dimension and population flows. Sociedad y Economía. 33, 145–174.

Vicente, A., Bravo-González, LA., López-Romero, A. et al. (2020). Craniofacial morphology in Down syndrome: A systematic review and meta-analysis. Scientific Reports, 10(1), 19895.

Wärmländer, S. K., Garvin, H., Guyomarc'h, P., Petaros, A., & Sholts, S. B. (2019). Landmark typology in applied morphometrics studies: What's the point? The Anatomical Record, 302(7), 1144-1153.

Wojcik, G. L., Graff, M., Nishimura, K. K., Tao, R., Haessler, J., Gignoux, C. R., Highland, H. M., Patel, Y. M., Sorokin, E. P., Avery, C. L., Belbin, G. M., Bien, S. A., Cheng, I., Cullina, S., Hodonsky, C. J., Hu, Y., Huckins, L. M., Jeff, J., Justice, A. E., … Carlson, C. S. (2019). Genetic analyses of diverse populations improves discovery for complex traits. Nature, 570(7762).

ACKNOWLEDGEMENTS

We are grateful for the voluntary collaboration of all participants, including children and their families. We are thankful to Colegio Ecológico Scout and Universidad Icesi for

granting us permission to organize the photographic sessions in Colombia. This study was funded by Proyecto COL0012168-1097 Interfacultades-ICESI, Beca predoctoral Fundación Álvaro Entrecanales-Lejeune to LME-Q, Joan Oró grant (2024 FI-3 00160) from the Recerca i Universitats Departament (DRU) of the Generalitat de Catalunya and the European Social Fund to AH-L, Wenner Gren Foundation for Anthropological Research (Gr. 10657), Agència de Gestió d'Ajuts Universitaris i de Recerca (AGAUR) of the Generalitat de Catalunya (2021 SGR00706 and 2021 SGR0139), and Biological Anthropological Master UB-UAB.

SUPPLEMENTARY INFORMATION

Supplementary table 1. Anatomic definition of the facial landmarks collected from the 3D models shown in Figure 1.

REFERENCE POINT	ANATOMICAL POSITION
1	**Glabellla:** midpoint between the eyebrows
2	**Sellion:** deepest point of the nasal root
3	**Pronasale:** most anterior point of the tip of the nose
4	**Subnasale:** point where the nasal septum meets the nasal groove
5	**Labiale Superius:** midpoint of the superior lip suture
6	**Labial Inferius:** midpoint of the inferior lip suture
7	**Endocación R:** inner lateral commissure point of the right eye
8	**Endocación L:** inner lateral commissure point of the left eye
9	**palpebral inferior R:** most inferior medial point of the right lower eyelid
10	**Exocanthion R:** outer lateral commissure point of the right eye
11	**palpebral inferior L:** most inferior medial point of the left lower eyelid
12	**Exocanthion L:** outer lateral commissure point of the left eye
13	**Subalare R:** facial insertion of the right alar base
14	**Subalare L:** facial insertion of the left alar base
15	**Chelion R:** point located at the right labial commissure
16	**Crista philtra R:** intersection of the vermilion line and the raised edge of the right nasolabial groove
17	**Crista philtra L:** intersection of the vermilion line and the raised edge of the left nasolabial groove
18	**Chelion L:** point located at the left labial commissure